Available online: journal.ipb.ac.id/index.php/jphpi

CHEMICAL COMPOSITION PROFILE, HEAVY METAL CONTENT, AND STRUCTURE OF *Ulva lactuca* AT MICRO AND NANO SCALES

Niken Dharmayanti[1], Ni Putu Tantri Miranti[1]*, Tatty Yuniarti[1], I Ketut Sumandiarsa[2], Muhammad Miftah Jauhar[3], Assyaffa Wafiqah[3], Ani Leilani[4], Aef Permadi[2], Resmi Rumenta Siregar[2], Khamhou Thongsamouth[5], Fera R Dewi[6]

[1]Fisheries Resources Utilization Study Program, Politeknik Ahli Usaha Perikanan Postgraduate
Pasar Minggu Street, South Jakarta, Jakarta, Indonesia 12520
[2]Fisheries Product Processing Technology Study Program, Politeknik Ahli Usaha Perikanan
Pasar Minggu Street, South Jakarta, Jakarta, Indonesia 12520
[3]Nano Center Indonesia,
Setu, South Tangerang City, Banten 15314
[4]Fisheries Extension Study Program, Politeknik Ahli Usaha Perikanan
Cikaret Street No. 2, Bogor, West Java, Indonesia 16132
[5]Department of Livestock and Fisheries, Ministry of Agriculture and Forestry
PO Box 6644, Vientiane Laos 01000
[6]Research Center for Applied Microbiology, National Research and Inovation Agency (BRIN)
B.J. Habibie Building, M.H. Thamrin Street No. 8, Central Jakarta Indonesia 10340

Submitted: 25 August 2025/Accepted: 7 April 2026
*Correspondence: tantrimiranti.aup@gmail.com

How to cite (APA Style 7th): Dharmayanti, N., Miranti, N. P. T., Yuniarti, T., Sumandiarsa, I. K., Jauhar, M. M., Wafiqah, A., Leilani, A., Permadi, A., Siregar, R. R., Thongsamouth, K., & Dewi, F. R. (2026). Chemical composition profile, heavy metal content, and structure of *Ulva lactuca* at micro and nano scales. *Jurnal Pengolahan Hasil Perikanan Indonesia,* 29(5), 375-397. http://dx.doi.org/10.17844/qebg1c85

Abstract

Ulva lactuca has high potential as a food source and bio-based industrial material. The effectiveness of its utilization varies greatly owing to its physical form and particle size. This study aimed to evaluate two particle forms of *U. lactuca*, namely micro and nano, based on chemical variables, heavy metal content, and particle structure in terms of functional groups, size, and morphology. The samples were milled using a Planetary Ball Mill into nanopowder. Chemical analysis included proximate composition, amino acid profile, heavy metal testing (Hg, Pb, Cd, and As), and particle structure using FTIR analysis, PSA measurements, SEM, and TEM. The ball milling process significantly affected the physicochemical characteristics and particle morphologies of the samples. The protein content increased from 4.69% to 6.47%, and the total amino acid content increased from 4.7% to 6.2%. Heavy metal concentrations remained below the limits established by the SNI 7383:2009. The Z-average value of 728.1±190.9 nm with a PDI of 0.53 indicates a polydisperse system with two particle populations (30 nm and 261 nm). SEM and TEM micrographs revealed that the nanopowder surface was more porous, containing spherical particles of 20–80 nm, indicating cell wall fragmentation and degradation of the ulvan polysaccharide matrix. Transforming *U. lactuca* into nanopowder enhances its functional value while preserving major functional groups, making it a promising natural raw material for food, pharmaceutical, and marine biotechnology applications.

Keywords: amino acid, nanopowder, SEM, TEM, Z-average value

http://dx.doi.org/10.17844/qebg1c85

Profil Komposisi Kimia, Kandungan Logam Berat dan Struktur *Ulva lactuca* pada Skala Mikro dan Nano

Abstrak

Ulva lactuca berpotensi tinggi sebagai sumber pangan dan bahan industri berbasis hayati. Efektivitas pemanfaatannya sangat variatif diakibatkan oleh bentuk fisik dan ukuran partikel. Penelitian ini bertujuan untuk mengevaluasi dua bentuk partikel dari *Ulva lactuca*, yaitu mikro dan nano berdasarkan variabel kimia, kandungan logam berat, dan struktur partikel berupa gugus fungsi, ukuran serta morfologi. Penggilingan sampel menggunakan *Planetary Ball Mill* menjadi nanopowder. Analisis kimia meliputi komposisi proksimat, profil asam amino, pengujian logam berat (Hg, Pb, Cd dan As) serta struktur partikel melalui analisis FTIR, pengukuran PSA, SEM dan TEM. Proses *ball milling* secara signifikan memengaruhi karakteristik fisikokimia dan morfologi partikel. Kandungan protein meningkat dari 4,69% menjadi 6,47% dan total asam amino naik dari 4,7% menjadi 6,2%. Logam berat masih berada di bawah ambang batas SNI 7383:2009. Nilai *Z-average* 728,1±190,9 nm dengan PDI 0,53 mengindikasikan sistem polidispers dengan dua populasi ukuran partikel (30 nm dan 261 nm). Citra SEM dan TEM menunjukkan permukaan *nanopowder* lebih berpori dengan partikel sferis berukuran 20–80 nm, menandakan terjadinya fragmentasi dinding sel dan degradasi matriks polisakarida ulvan. Secara keseluruhan, transformasi *Ulva lactuca* menjadi *nanopowder* meningkatkan nilai fungsional biomassa tanpa mengubah gugus fungsi utama, menjadikannya kandidat potensial sebagai bahan baku alami untuk aplikasi pangan, farmasi, dan bioteknologi kelautan.

Keywords: asam amino, *nanopowder*, nilai *Z-average*, SEM, TEM

INTRODUCTION

Ulva lactuca, commonly known as *sea lettuce*, is a type of green macroalgae (*Chlorophyta*) commonly found in the coastal areas of Indonesia. This type of algae is known to have a fast growth rate and high adaptability to various aquatic environments (Hayati *et al*., 2023). These advantages make *U. lactuca* a potential candidate for the development of bio-based bioproducts for food, feed, pharmaceutical, and environmental applications. Various studies have explored the potential of *U. lactuca* as a source of high-value biological biomass. Previous studies have shown that *U. lactuca* contains various bioactive components, such as polysaccharides, proteins, essential amino acids, pigments, and antioxidant and antimicrobial compounds, which are beneficial for health (Costa *et al*., 2018; Shuuluka *et al*., 2013). Seaweeds possess a complex chemical profile rich in polysaccharides, proteins, pigments, minerals, and phenolic compounds, which underpin their nutritional and functional properties (Holdt & Kraan, 2011). However, macroalgae are also known to accumulate trace elements and heavy metals from surrounding waters through functional groups in their cell wall polysaccharides, making them widely studied as bioindicators and potential agents for bioremediation (Akbar *et al*., 2025). These dual characteristics highlight the importance of evaluating both the chemical composition and heavy metal content when seaweed biomass is intended for food, pharmaceutical, or health-related applications.

However, the effectiveness of bioactive compounds in natural foods is strongly influenced by their physical form and the processing methods used. Overly complex and industrially based processing tends to decrease the nutritional quality and biological activity of food ingredients. According to the FAO report in the NOVA food classification system (Monteiro *et al*., 2019), the consumption of ultra-processed *foods* (NOVA group 4) is significantly associated with reduced diet quality and an increased risk of non-communicable diseases. Therefore, processing approaches based on unprocessed or minimally processed foods (NOVA group 1), such as drying, milling, and size reduction

without the addition of synthetic additives, are important strategies for maintaining the natural benefits of foods such as *U. lactuca*. One of the current approaches is the reduction of particle size to nanopowder. This process can increase the specific surface area of the particles, which affects the solubility, stability, and bioavailability of bioactive compounds (Hanutami & Budiman, 2018). Thus, the functional compounds in *U. lactuca* could potentially be more effectively absorbed by the body when consumed as nanopowder than as regular powder.

Several previous studies have shown that the particle size of raw materials affects the bioavailability of active compounds and the functional performance of the final product. Sari *et al*., (2016) mentioned that the antioxidant activity of natural material-based compounds is largely determined by the size of the particles produced, particles with smaller sizes show an increase in surface area which tends to have higher effectiveness. Sianipar *et al*., (2022) reported that the smaller particle sizes enhance extraction efficiency by improving solvent penetration and diffusion into the solid. Similarly, Indah *et al*. (2021) showed that particle size significantly affects the metal adsorption capacity of *Gracilaria* sp. powder, indicating that an increased surface area facilitates interactions between solids and the surrounding media. An increase in the mesh size indicates a decrease in the adsorbent particle size. The smaller the adsorbent particle size, the higher was the magnesium absorption efficiency. Raya and Rahmah (2012) mentioned that this phenomenon is closely related to the specific surface area of the adsorbent, where a larger surface can provide more active sites to bind metal ions. A large surface area is generally associated with a fine pore structure; the smaller the pore size, the larger the total surface area, thus increasing the adsorption ability of magnesium ions. In addition, structural analyses using FTIR, SEM, and TEM have been used to evaluate the physicochemical changes due to mechanical treatment (Rasyida *et al*., 2019). However, studies that explicitly examine the relationship between particle size and chemical composition, structural characteristics, and heavy metal profiles in an integrated manner are limited.

Despite the increasing interest in nanoparticle-based processing of marine biomass, the scientific implications of particle size reduction on the intrinsic chemical composition and safety profile of macroalgal materials remain unclear. In particular, the mechanochemical effects of high-energy ball milling may not only modify particle morphology but also potentially influence the detectability, distribution, and release of heavy metals bound within the cell wall matrix. While previous studies have reported improvements in extraction efficiency and bioactive compound availability following particle size reduction, integrated investigations linking particle size transformation with the chemical composition, structural characteristics, and heavy metal profiles in *U. lactuca* are still limited. This knowledge gap is important because nanoparticle formation may simultaneously enhance bioavailability while altering the exposure of trace metal contaminants in the environment. Therefore, a comprehensive evaluation is required to clarify whether mechanical nanosizing modifies the chemical integrity, structural properties, and heavy metal distribution of *U. lactuca* biomass for food and nutraceutical applications.

Despite extensive research on the effects of particle size in plant-based materials and other seaweed species, integrated studies that simultaneously evaluate the impact of particle size reduction on the chemical composition, material structure, and heavy metal distribution in *U. lactuca* remain scarce. The novelty of this study lies in the integrated evaluation of the physicochemical consequences of particle size reduction in *U. lactuca* biomass at both the micro-and nanoscale levels. Unlike previous studies that primarily focused on extraction efficiency or single compositional parameters, this study simultaneously investigated the relationship between particle size transformation, chemical composition, heavy metal distribution, and structural characteristics using complementary analytical techniques (proximate analysis, amino acid profiling, ICP-MS, FTIR, PSA, SEM, and TEM). This

http://dx.doi.org/10.17844/qebg1c85

integrated approach provides new insights into how mechanochemical processing influences the nutritional value, safety, and structural integrity of macroalgal biomass. The findings of this study provide important scientific evidence for the safe and efficient utilization of macroalgal biomass processed into nanopowder, contributing to the development of marine-based functional ingredients and biomaterials. The results of this study are expected to provide a scientific basis for determining *U. lactuca* processing strategies that are more efficient, safe, and high value-added. This research is important for the marine biota-based food, pharmaceutical, and cosmetic industries, supporting efforts to utilize marine resources sustainably. From a safety perspective, understanding the heavy metal profile in relation to particle size will help formulate process limitations that comply with food and health quality standards. This study aimed to evaluate the effects of two forms of *U. lactuca* particles, micro and nano, on chemical variables, heavy metal content, and particle structure, including morphology, size, and functional groups.

MATERIALS AND METHODS

Powder and Nanopowder Preparation

The main material used was *U. lactuca* seaweed obtained from the coast of Seriwe Village, Jerowaru District, East Lombok Regency, Nusa Tenggara Barat Province (coordinates 8°53'18.6" S and 116°30'27.8" E). The sampling location map of *U. lactuca* is shown in Figure 1. *Ulva lactuca* seaweed was washed using seawater, drained, and stored in a styrofoam box equipped with ice flakes as a container during the transportation process, which was then washed again using freshwater to remove any remaining sand, dirt, and other impurities still attached to the thallus. *U. lactuca* was then dried using a Getra low-pressure gas oven (NFC-8Q) for 48 h at 35°C (Moreira *et al*., 2017; Fithriani *et al*., 2017).

Ulva lactuca seaweed was dried and then mashed using a grinder (BRANDT brand), and then the sieving process sieved using a 40 mesh sieve, based on specifications from the industry. The size was then reduced to nanoparticles using a planetary ball mill (DECO-PBM-V-60L brand) with a top-down method for 12 h with 1 in total, each step includes 10-15 minutes (on) and 10-15 minutes (off), and the speed used was 400-700 rpm. The milling speed and time were optimized according to the characteristics of the material. The process flow of the *U. lactuca* nanopowder is shown in Figure 2.

Proximate Analysis

Proximate analysis was carried out to determine the moisture content by the

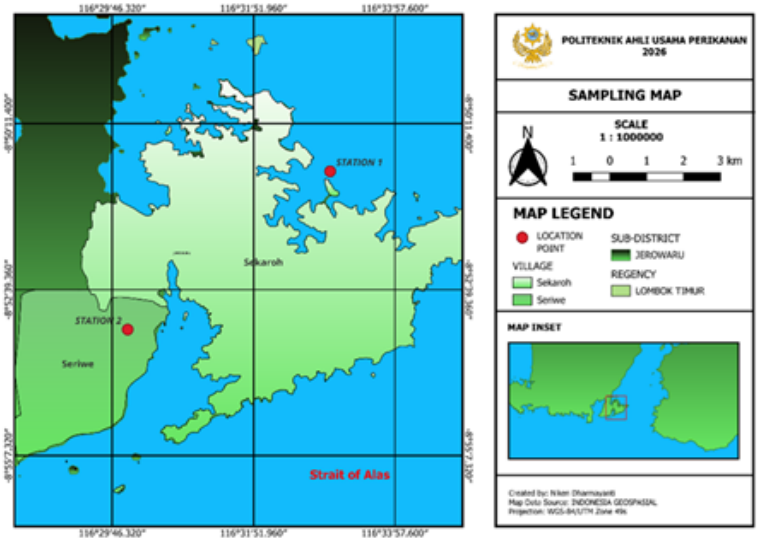

Figure 1 Sampling site of *Ulva lactuca* seaweed in Seriwe Village, Jerowaru District, East Lombok Regency, Nusa Tenggara Barat Province

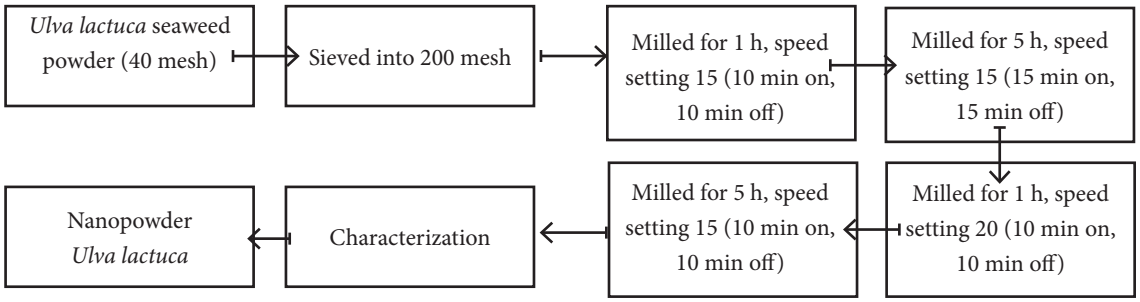

Figure 2 Flow diagram of the nanopowder processing steps

gravimetric method (Badan Standardisasi Nasional [BSN], 2015), ash content by the gravimetric method (BSN, 2010), fat content by the Soxhlet method (BSN, 2017), protein content by the *Kjeldahl* method (BSN, 2006), and carbohydrate content by the Carbohydrate by Difference method.

Amino Acid Profile Analysis

Amino acid analysis was performed using high-performance liquid chromatography (HPLC) with fluorescence detection after pre-column derivatization using o-phthalaldehyde (OPA) at the Laboratory of the IPB University, Bogor. A total of 6 mg of protein from each sample was hydrolyzed with 2 mL of 6 N HCl in a screw-cap tube under a nitrogen atmosphere and incubated at 110°C for 24 h. The hydrolysate was then evaporated to dryness using a rotary evaporator, reconstituted with 10 mL of 0.01 N HCl, and filtered through a 0.45 µm membrane filter before derivatization. The OPA reagent was prepared by mixing 25 mg of OPA, 2 mL of methanol, 0.02 mL of 2-mercaptoethanol, 0.05 mL of Brij-30, and 0.5 mL of 1 M borate buffer (pH 10.4), followed by dilution with borate buffer (1:2, v/v) prior to use. Subsequently, 5 µL of the sample solution was reacted with 25 µL of the OPA reagent for one minute at room temperature to ensure complete derivatization. After derivatization, 5 µL of the mixture was injected into the HPLC column, and chromatographic separation was performed for approximately 25 min. The analytical conditions for HPLC were as follows:

Mobile phase : Thermo Scientific ODS-2 Hyersil
Flow rate : Buffer A and buffer B using a gradient elution system
Detector : Fluorescence

Heavy Metal Analysis

Heavy metal analysis was conducted using inductively coupled plasma-mass spectrometry (ICP–MS) at the Saraswanti Indo Genetech Laboratory. Sample preparation for heavy metal analysis was performed by establishing a six-point standard calibration curve. For the determination of mercury (Hg), lead (Pb), and cadmium (Cd), approximately 0.25 g of the sample was subjected to wet digestion using a mixture of concentrated HNO_3 and H_2O_2 to ensure complete mineralization of the sample. For arsenic (As) analysis, the sample was treated with concentrated HCl, dilute hydrazine sulfate solution, and HBr-p solution, followed by chloroform extraction. The obtained extract was then evaporated with HNO_3 until nearly dry, redissolved in HCl, and treated with a reducing agent mixture of KI and ascorbic acid to stabilize the As species prior to instrumental analysis.

Structure Characterization

Characterization was carried out using a particle size analyzer (Beckman Coulter) to determine the size of the particles produced. Measurements were conducted under optimized dispersion conditions, employing deionized water containing 2% sodium polyphosphate as the dispersant, a sample concentration of 0.01 ppm, and 1-minute sonication at ambient temperature. Fourier Transform Infrared (FTIR) spectroscopy (Smart iTX Accessory type) was used to determine the functional groups present. Scanning Electron Microscopy (SEM; JEOL-6510 LA) and Transmission Electron

http://dx.doi.org/10.17844/qebg1c85

Microscopy (TEM; Tundra 100 kV) were used to observe the surface morphology of the resulting powder. Approximately 2 g of *U. lactuca* powder and nanopowder were placed on circular copper plates (sample holders) before microscopic observation. The microstructure was examined at magnifications of 500×, 5,000×, and 10,000×, with the measurements performed under an accelerating voltage of 20 kV.

Data Analysis

The experimental data were analyzed using an Independent Samples *t*-test to determine significant differences between the two treatments, *U. lactuca* powder (micro) and nanopowder (nano), in terms of chemical composition (proximate and amino acid profile) and heavy metal content (Hg, Pb, Cd, and As). The analysis was performed in two replicates. Statistical significance was assessed at a confidence level of $p<0.05$ to evaluate the existence of meaningful differences between treatments. Prior to the *t*-test, the data were examined for normality and homogeneity of variance to ensure compliance with the parametric test assumptions. Statistical analyses were performed using the IBM SPSS Statistics software. The results are expressed as mean ± standard deviation (SD). Additionally, supporting data from PSA, SEM, TEM, and FTIR analyses were interpreted descriptively to evaluate the changes in morphological structure, particle size, and functional groups between the powder and nanopowder samples. The quantitative and qualitative results were comprehensively integrated to elucidate the relationship between particle size reduction, chemical composition variations, and functional potential of *Ulva lactuca* biomass.

RESULT AND DISCUSSION

Chemical Composition of *U. lactuca* Powder and Nanopowder

The proximate composition between the particle size of *U. lactuca* powder and nanopowder (Table 1) exhibited statistically significant differences ($p<0.05$) in several parameters, reflecting the compositional and structural modifications induced by the dry ball milling process.

In this study, dried *U. lactuca* was first ground to 40 mesh using a mechanical grinder, followed by high-energy dry ball milling without any solvent addition until the particle size reached the nanoscale. Unlike wet milling, the absence of a liquid medium during this process causes high-frequency particle–particle and particle–wall collisions, which generate localized frictional heat and strong shear forces. These mechanical stresses are known to induce changes in the physicochemical properties of biopolymers, such as fragmentation, surface oxidation, and molecular rearrangements (Loh *et al.*, 2015).

The moisture content of *U. lactuca* showed a significant increase from 7.38±0.32% in micron particles (powder) to 14.27±0.17% after ball milling. This increase indicates a greater water retention capacity resulting from the finer particle size and more porous particle structure. The top-down milling process breaks down large aggregates into nanoscale particles, substantially expanding the specific surface area and increasing the number of micro- and nanopores in the material. These structural changes facilitate the easier penetration of water molecules into the particle matrix and enhance the overall water adsorption capacity (Monks *et al.*, 2013).

Table 1 Chemical composition of *U. lactuca* powder dan nanopowder

Parameters (%)	*U. lactuca* powder	*U. lactuca* nanopowder
Moisture	7.38±0.32[a]	14.27±0.17[b]
Ash	31.61±0.37[b]	28.77±0.39[a]
Lipid	2.38±0.33[b]	1.30±0.25[a]
Protein	4.69±0.11[a]	6.47±0.17[b]
Carbohydrate (by differences)	53.94±0.58[b]	49.19±0.52[a]

Numbers with distinct superscript letters (a, b) differ significantly ($p<0.05$).

Zhao *et al*. (2024) reported that smaller hydrogel particles (with a higher specific surface area) significantly increased the water holding capacity (WHC) and physically adsorbed water (PAW) compared to larger particles. In addition to the increased surface area, the rise in moisture content in the *U. lactuca* nanopowder is closely related to the enhanced hygroscopicity and surface energy induced by structural transformations during dry milling. The high mechanical energy generated during ball milling leads to the partial amorphization of cell wall polysaccharides, such as ulvan, cellulose, and hemicellulose. This amorphous transformation exposes hydroxyl (-OH) and carboxyl (-COOH) functional groups that have a strong affinity for atmospheric water molecules (Jung *et al*., 2018).

The ash content represents the inorganic mineral fraction remaining after the complete combustion of the sample. In this study, *U. lactuca* nanopowder exhibited a lower ash content (28.77 ± 0.39%) than its powdered form (31.61 ± 0.37%). Rather than mineral volatilization, in the study by Chan *et al*. (2018), this reduction is more likely attributable to the mechanical redistribution and partial loss of loosely bound minerals during prolonged ball milling, as well as increased adhesion of ultrafine particles to the milling media and container surfaces, which may reduce mineral recovery during ash determination.

The lipid and protein contents were significantly higher in the *U. lactuca* nanopowder than in the powder. This increase was attributed to intensified cell wall disruption during prolonged ball milling, which enhanced the release and extractability of intracellular lipid fractions and previously inaccessible protein components. Mechanical forces, such as shear stress, impact, and friction during milling, promote the cracking of the polysaccharide-rich cell wall matrix, thereby exposing both hydrophobic domains associated with lipid bodies and hydrophilic protein structures (Spínola *et al*., 2023).

The lipid content in powder and nano forms was similar to the results of previous studies, which showed that *Ulva lactuca* composition generally contains 0.5-4% lipid and 5-27% protein, indicating that the pulverization process enriches the availability of these macro compounds (Metwaly *et al*., 2023). A notable decrease in the lipid content from 2.38 ± 0.33% to 1.30 ± 0.25% was observed after the transition from powder to nanopowder. This reduction is primarily attributed to the oxidative and thermal degradation of unsaturated fatty acids resulting from high-energy impact collisions during dry ball milling (Lam *et al*., 2001).

In contrast, the protein content exhibited a significant increase from 4.69 ± 0.11% to 6.47 ± 0.17% after milling treatment. The ball milling process promotes the solubilization of intracellular proteins and facilitates their interaction with analytical reagents, which may lead to higher protein concentrations. Additionally, compositional shifts caused by lipid loss and moisture absorption can increase the relative proportion of protein when expressed on a wet weight basis. The heat generated during milling can cause partial denaturation or mild Maillard-type reactions, as explained by Khalid *et al*. (2023), who stated that these reactions can change the nitrogen content and cause a significant increase in the measured protein values.

Furthermore, the carbohydrate composition of nano and powder, which is the difference of 100% proximate results (by difference), shows that the smaller particles contain lower carbohydrates (49.19% nano and 53.94% powder). Polysaccharides are one of the constituents of carbohydrates, which are generally related to the fiber in a material (Nufus *et al*., 2017). Polysaccharides, particularly ulvan, remain the dominant carbohydrate fraction in *U. Lactuca* (approximately 48%), indicating that the main polysaccharide structure is largely preserved after milling (Li *et al*., 2023).

However, a lower carbohydrate content was observed in the nanopowder than in the powder. This decrease should not be interpreted as extensive polysaccharide degradation but is mainly associated with proximate analysis by difference, where increased protein and

http://dx.doi.org/10.17844/qebg1c85

lipid extractability after intensive milling mathematically reduces the calculated carbohydrate fraction (Patrichi *et* al., 2023). Furthermore, prolonged ball milling promotes the mechanical disruption of the ulvan-rich cell wall matrix, which may induce partial mechanochemical depolymerization and structural rearrangement of polysaccharides. These effects can influence polysaccharide distribution, solubility, and analytical recovery without causing a complete loss of ulvan. The literature states that carbohydrates in *Ulva* range from 53-78 % depending on environmental factors and extraction methods (Hofmann *et al*., 2024).

Amino Acid Profile

Amino acid analysis of the powder and nano samples revealed 15 types of amino acids with different compositions. The total amino acid content increased from 4.7% in the powder to 6.2% in the nanopowder, aligning with the corresponding rise in protein content (from 4.69% to 6.47%).

The difference in composition or total amount of amino acids may arise due to the thermal or oxidative degradation of some amino acids during processing. The ball milling process, which involves intensive friction, generates heat, thus causing a decrease in the amino acid content in the nanopowder. Jacoeb *et al*. (2012) mentioned that some amino acids are susceptible to heat damage, which results in a reduction in the amount of amino acids. The results of the amino acid analysis of *U. lactuca powder* and nanopowder are presented in Table 2.

U. lactuca seaweed contains essential (threonine, valine, isoleucine, leucine, phenylalanine, histidine, lysine, and arginine) and non-essential (aspartic acid, serine, glutamate, glycine, alanine, valine, tyrosine,

Table 2 Amino acid composition of *U. lactuca* powder and nanopowder

Amino acid type	*U. lactuca* powder (%w/w)	*U. lactuca* nanopowder (%w/w)
Essential amino acids		
Phenylalanine	0.32±0.06[a]	0.27±0.00[a]
Isoleucine	0.60±0.00[b]	0.30±0.00[a]
Valin	0.48±0.00[b]	0.22±0.01[a]
Arganine	0.18±0.01[a]	0.70±0.01[b]
Lysine	0.35±0.01[b]	0.12±0.01[a]
Leucine	0.65±0.07[a]	0.48±0.02[a]
Threonine	0.25±0.07[a]	0.33±0.00[a]
Histidine	0.19±0.00[a]	0.26±0.01[b]
Total essential amino acids	3.02[a]	2.68[b]
Non-essential amino acids		
Serine	0.14±0.00[a]	0.38±0.00[b]
Glutamic acid	0.52±0.00[a]	0.77±0.01[b]
Alanine	0.29±0.01[a]	0.58±0.01[b]
Glycine	0.16±0.01[a]	0.37±0.02[b]
Aspartic acid	0.27±0.01[a]	0.83±0.01[b]
Tyrosine	0.18±0.01[a]	0.26±0.01[b]
Proline	0.14±0.02[a]	0.38±0.00[b]
Total non-essential amino acids	1.7[a]	3.57[b]
TOTAL amino acids	4.7[a]	6.2[b]

Numbers with distinct superscript letters (a, b) differ significantly ($p<0.05$).

and proline) amino acids. According to Shuuluka *et al*. (2013), *Ulva* sp. generally has a total free amino acid content between 2-5%, depending on the harvest season and extraction method, so these results are in line. Research on the amino acid content of different Ulva species by Meiyasa *et al*. (2023) showed that *U. reticulata* has the same amino acid content with different compositions.

Based on the data in Table 2, mechanical milling significantly influenced the total amino acid content of *Ulva lactuca.* As the amino acid analysis involved an acid hydrolysis step prior to HPLC quantification, the measured values represent total amino acids, including both protein-bound and free amino acid fractions. The observed increase in the total amino acid content is attributed to the enhanced accessibility and analytical recovery of amino acids resulting from cell wall disruption and protein matrix disintegration during milling.

This observation agrees with that of Wang *et al*. (2024), who reported that when proteins are ball-milled, the protein particle size changes, and the particle size may be reduced under mechanical forces. As a result, the protein or particles through high-energy milling enhances the release of amino acid-rich peptides and soluble nitrogen compounds through shear stress, localized heating, and oxidative microenvironments. However, some compositional differences may also result from the thermal or oxidative degradation of heat-sensitive amino acids (Pratama *et al*., 2013) during ball milling. Sailah and Miladulhaq (2021) noted that such conditions can reduce certain amino acid levels through degradation or Maillard-type reactions with reducing sugars.

The data show that glutamic acid has the highest content in nanopowder form (0.77 %), far exceeding other amino acids. Glutamic acid, together with aspartic acid, is responsible for the savory (umami) taste typical of seaweed. This is in line with Meiyasa *et al*. (2023), who showed that *Ulva* sp. is rich in flavor-forming amino acids, especially aspartate and glutamate, which makes it a potential natural flavor enhancer. This decrease may affect the taste and *flavor* potential, although in terms of bioavailability, nanosized particles may increase amino acid absorption in the gastrointestinal tract.

The total EAA content slightly decreased in the nanopowder (2.68%) compared to that in the powder (3.02%), whereas the NEAA content increased markedly from 1.7% to 3.57%. This trend suggests that while some EAAs, such as valine, isoleucine, and lysine, were partially degraded due to heat or oxidation, other amino acids, especially aspartic acid, glutamic acid, alanine, and serine, increased due to enhanced protein breakdown and hydrolysis. Interestingly, some essential amino acids, such as arginine, threonine, and histidine, increased in the nanopowder form. This increase could be due to the effect of greater protein release from the *Ulva lactuca* cell matrix when pulverized to nanosized particles, making certain amino acids more detectable in the analysis. These essential amino acids play important roles in physiological functions; for example, threonine plays a crucial role in maintaining the integrity and function of the gastrointestinal mucosal layer (Mao *et al*., 2011). This decrease, along with the decrease in total amino acids in the nanopowder, indicates the degradation of some proteins due to heat, oxidation, or changes in molecular structure during the refining process.

Nutritionally, *Ulva lactuca* in both powder and nanopowder forms offers a complete spectrum of amino acids, making it a potential candidate as a raw material for food, pharmaceutical, and health applications. Similar essential amino acid profiles of *U. lactuca* have been reported by Pratiwi *et al*. (2021), supporting its nutritional relevance as a plant-based protein source.

Heavy Metal Profile

Heavy metal analysis of *Ulva lactuca* revealed distinct differences in concentration between the powder and nanopowder forms (Table 3). The analyzed parameters included mercury (Hg), lead (Pb), arsenic (As), and cadmium (Cd). The mercury content decreased from 0.05±0.00 mg/kg in the powder to 0.03±0.00 mg/kg in the nanopowder, whereas the Pb and As concentrations increased from 0.72±0.01 mg/kg to 1.06±0.03 mg/kg and

http://dx.doi.org/10.17844/qebg1c85

Table 3 Heavy metal analysis results of *U. lactuca* powder and nanopowder

Parameters	*U. lactuca* powder (mg/kg)	*U. lactuca* nanopowder (mg/kg)	Standard (SNI 7383:2009) (mg/kg)
Mercury (Hg)	0.05±0.00[b]	0.03±0.00[a]	0.5
Lead (Pb)	0.72±0.01[a]	1.06±0.03[b]	Max. 10
Arsenic (As)	0.28±0.00[a]	0.82±0.01[b]	1.0
Cadmium (Cd)	0.07±0.00[a]	0.08±0.01[a]	0.2

Numbers with distinct superscript letters (a, b) differ significantly (p<0.05).

from 0.28±0.00 mg/kg to 0.82±0.01 mg/kg, respectively.

Meanwhile, Cd levels remained relatively stable between 0.07–0.08 mg/kg. Despite these variations, all measured values were well below the maximum permissible limits established by SNI 7387:2009, namely, 0.5 mg/kg for Hg, 10 mg/kg for Pb, 1.0 mg/kg for As, and 0.2 mg/kg for Cd. Therefore, both *Ulva lactuca* powders and nanopowders are considered safe for consumption and comply with national food safety standards.

The reduction of mercury (Hg) in the nanopowder is likely due to its high volatility during ball milling. According to Vassilev *et al.* (2024), mercury exhibits a high volatilization rate (83–99%) during thermal treatment. Frictional heat and localized temperature elevation inside the milling chamber may induce partial vaporization or transformation of Hg into a gaseous form, thereby reducing its detectable concentration in the final product. This finding aligns with Liu *et al.* (2024), who reported that mechanical and thermal processing can promote the volatilization of mercury from marine biomass. Furthermore, the physicochemical nature of mercury supports this behavior, as it exists as a liquid metal with a low vapor pressure (2 mmHg) and a low latent heat of evaporation (295 kJ/kg), making it susceptible to vaporization even at ambient temperatures (Veeraswamy *et al.*, 2023). Consequently, frictional heating or localized thermal stress during milling can significantly enhance mercury volatilization from the biomass matrices.

Conversely, the increase in Pb and As concentrations in the nanopowder may be attributed to the greater specific surface area generated after the particle size reduction. Nanoparticles exhibit a higher adsorptive capacity, allowing heavy metal ions such as Pb^{2+} and As^{3+} to bind more effectively to negatively charged functional groups, particularly carboxyl (-COOH) and hydroxyl (-OH) groups, on cell wall polysaccharides (Safitri, 2020). Moreover, the broader dispersion of mineral fractions in the nanopowder can facilitate the detection of heavy metals previously entrapped within the cell wall matrix during ICP-MS analysis. Indah *et al.* (2021) showed that the particle size of the adsorbent affects the adsorption process; the smaller the size of the adsorbent, the higher the absorption of metals. These results are reinforced by Raya and Rahmah (2012), who stated that a wider specific surface of the adsorbent can provide more active sites to bind metal ions. A large surface area is generally associated with a fine pore structure; the smaller the pore size, the greater the total surface area, and the greater the adsorption ability of magnesium ions.

Overall, these findings indicate that ball milling not only alters the physical and chemical properties of *Ulva lactuca* particles but also affects the behavior of heavy metals in the biomass matrix. The reduction in Hg reflects partial volatilization due to mechanical-thermal effects, whereas the increase in Pb and As represents a redistribution of metals from bound to more detectable forms. Nevertheless, all values complied with SNI 7387:2009 and FAO/WHO (2019) international safety standards, confirming the safe utilization of *Ulva lactuca* nanopowder for food and nutraceutical applications.

Structure Characterisation Fourier tranform infrared spectroscopy (FTIR)

Fourier transform infrared (FT-IR) analysis was used to evaluate whether the particle size reduction altered the main functional groups of *U. lactuca,* allowing a comparison between the powder and nanopowder samples. The FTIR characterization results are presented in Figure 3 and Table 4.

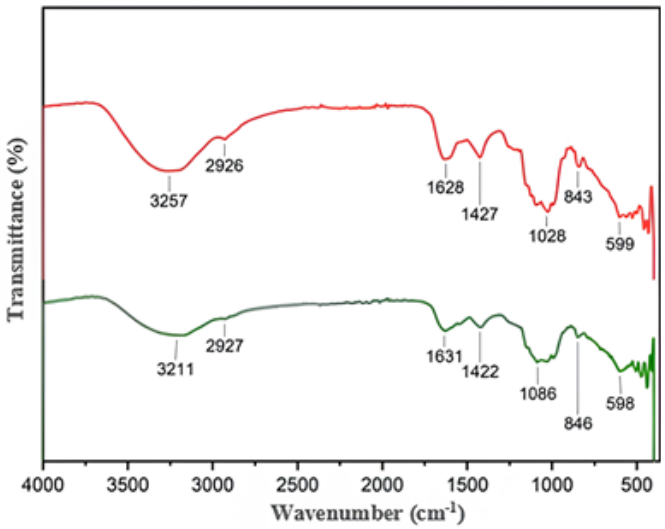

Figure 3 FTIR spectrum analysis of *U. lactuca* powder (—) and nanopowder (—)

Table 4 FTIR spectral interpretation of *U. lactuca* powder and nanopowder

No	Chemical bond present in *Ulva lactuca*	Observed wavelength (cm^{-1})
Before processing (powder)		
1	O-H hydroxyl stretching	3,211
2	C-H alkane stretching	2,927
3	C=C alkane	1,631
4	O-H bending carboxylic acid	1,422
5	C–O stretching (carbohydrates/polysaccharides)	1,086
6	C–H bending (out-of-plane bending of =C–H on aromatic or alkenes)	846
7	C–Br or C–Cl stretching (halogenated compounds)	598
After processing (nanopowder)		
1	O-H hydroxyl stretching	3,257
2	C-H alkane stretching	2,926
3	C=C alkane	1,628
4	O-H bending carbocylic acid	1,427
5	C–O stretching (carbohydrates/polysaccharides)	1,028
6	C–H bending (out-of-plane bending of =C–H on aromatic or alkenes)	843
7	C–Br or C–Cl stretching (halogenated compounds)	599

http://dx.doi.org/10.17844/qebg1c85

The FTIR spectra of *U. lactuca* powder and nanopowder exhibited characteristic ulvan-related bands, including sulfate ester, carboxylate, and glycosidic vibrations. The slight peak shifts and intensity variations observed after milling reflect changes in the intermolecular interactions and molecular organization induced by particle size reduction, without evidence of covalent bond degradation. Ramadhan *et al*. (2022) reported that hydroxyl (O–H) and C–H stretching vibrations are the principal absorption bands observed in polysaccharides. Table 4 shows a broad absorption band at 3,211 cm ^{1} (powder) and 3,257 cm ^{1} (nanopowder), corresponding to O–H stretching vibrations, which are the main features of the polysaccharide backbone owing to extensive hydrogen bonding among hydroxyl and carboxyl groups. The slight shift to a higher wavenumber indicates an increase in the O–H bond energy caused by alterations in the hydrogen bonding environment following nanopowder formation.

This phenomenon can be attributed to the increase in surface area and the partial disruption of intramolecular hydrogen bonds. The absorption band at 2,926-2,927 cm ^{1}, assigned to C–H stretching vibrations (–CH_2, –CH_3), remained stable after the size reduction from powder to nanopowder. This stability is expected because these aliphatic C–H bonds are part of the polysaccharide backbone and side chains of ulvan, which are covalent bonds with high bond dissociation energies and are not readily cleaved under ambient mechanical milling conditions (Barakat *et al*., 2022). Mechanical milling primarily affects particle size and intermolecular interactions rather than breaking stable covalent C-H linkages, resulting in a preserved aliphatic fingerprint in the FTIR spectra (Zeng *et al*., 2018).

The absorption bands at 1,631 cm ^{1} (powder) and 1,628 cm ^{1} (nanopowder) are attributed to the asymmetric stretching vibrations of deprotonated carboxylate groups (–COO) arising from uronic acid residues, such as glucuronic and iduronic acids, in the ulvan polysaccharides. This assignment is consistent with the FTIR analyses of ulvan from *Ulva* species, where the bands near 1640 cm ^{1} were attributed to the COO asymmetric stretch and weaker bands around 1,438 cm ^{1} to the COO asymmetric stretch, reflecting the presence of uronic acid residues in the polysaccharide structure (Garcia *et al*., 2023).The relatively minor shift observed in this region indicates a slight change in the hydrogen bonding environment between the carboxylate and neighboring hydroxyl groups, rather than any cleavage of covalent bonds. This is more appropriately attributed to conformational rearrangements of uronic acid residues induced by particle size reduction during nanopowder formation, and such mechanical processing primarily affects inter- and intramolecular hydrogen interactions while preserving the integrity of the polysaccharide carbon backbone (Tran *et al*., 2023). These results support the conclusion that nanoparticle processing can modify intramolecular interactions without destroying the main carbon framework of polysaccharides.

The most significant change was observed in the absorption bands corresponding to the C-O and C-O-C stretching vibrations (the polysaccharide fingerprint region), which shifted from 1,086 cm ^{1} (powder) to 1,028 cm ^{1} (nanopowder). This region is characteristic of glycosidic linkages and secondary alcohol (C–O) vibrations from rhamnose and glucuronic acid residues (Ramadhan *et al*., 2022). The observed shift to a lower wavenumber did not provide direct evidence of glycosidic bond cleavage. Instead, such minor FTIR band shifts are more appropriately interpreted as changes in the hydrogen bonding environment and the conformation of glycosidic linkages due to physical processing, such as particle size reduction during the formation of the nanopowder. Infrared spectroscopy reflects alterations in inter- and intramolecular interactions and molecular packing rather than covalent bond breakage, and small wavenumber shifts within the glycosidic region often correlate with conformational adjustments or hydrogen bond rearrangements in polysaccharide chains without actual cleavage of the primary glycosidic bonds (Hong *et al*., 2021). Tran *et al.* (2023), who observed that physical treatments such as

sonication or grinding caused downward shifts in C–O stretching peaks of ulvan due to an increased number of free terminal hydroxyl groups (–OH). Therefore, this shift cannot be attributed to instrumental variation, as it is accompanied by changes in sulfate and uronate band intensities, suggesting genuine alterations in the micromolecular structure of ulvan.

In addition to hydroxyl and carboxyl groups, sulfate groups (–OSO_3) are the most distinctive functional features of ulvan and warrant an in-depth discussion. The strong bands observed at approximately 1,220–1,260 cm ^{1} (S=O stretching, sulfate ester) and 843–846 cm ^{1} (C–O–S stretching) confirm the presence of sulfate groups linked to rhamnose or iduronic backbones (Figueira *et al*., 2020). The relative intensity of sulfate to sugar bands (A_{1220}/A_{1050}) correlates with the degree of sulfation (DS). In the nanopowder spectrum, the sulfate bands appeared slightly weakened and shifted to lower wavenumbers. Such changes in intensity and position are more appropriately interpreted as reflections of alterations in the local bonding environment and intermolecular interactions of the sulfate ester groups rather than evidence of sulfate group removal or cleavage of covalent C-O-S bonds (Je *et al*., 2021).Infrared spectroscopy is sensitive to changes in molecular orientation, hydrogen bonding, and packing, which can influence the vibrational characteristics of sulfate esters in sulfated polysaccharides, as reported in studies of fucoidan and other sulfated polysaccharides, where shifts and intensity variations of the S=O stretching bands occur without implying desulfation (Ptak *et al.,* 2021). As sulfate groups play a critical role in determining the biological activity of ulvan, particularly its antioxidant and antidiabetic effects, these subtle changes should be noted as potential indicators of bioactivity modification following nanoparticle processing.

Overall, the FTIR spectral pattern of *U. lactuca* in this study was consistent with previous reports describing the characteristic bands of ulvan at approximately 3,400 cm ^{1} (O–H), 2,920 cm ^{1} (C–H), 1,620 cm ^{1} (C=O), 1,415 cm ^{1} (COO), 1,250 cm ^{1} (S=O), 1,060–1,030 cm ^{1} (C–O/C–O–C), and 845 cm ^{1} (C–O–S) (Barakat *et al*., 2022; Ibrahim *et al*., 2022). Minor variations in the peak position and intensity after processing indicate that the fundamental polysaccharide structure remained intact, although modifications in substituent groups and hydrogen bonding interactions occurred.

Particle Size Analyzer (PSA)

The PSA characterization results showed that the powder sample was not detected because the particle size (±100 μm) exceeded the maximum limit of the device (10 μm). During the griding process, *U. lactuca* is dried in a grinder to a size of 40 mesh or 420 microns in accordance with industry demand standards as a raw material for seasonings in both snack and non-snack products (PT. Indesso Culinaroma). Figure 4 shows the images of *Ulva lactuca* seaweed that were ground into powder using a grinder and subsequently subjected to further size reduction using a Planetary Ball Mill (PBM). The particle size data of the resulting nanopowder samples are presented in Table 5.

Particle size analysis performed using a Particle Size Analyzer (PSA) revealed that *Ulva lactuca* samples subjected to ball milling exhibited an average hydrodynamic diameter (Z-average) of 728.1±190.9 nm, with a polydispersity index (PDI) of 0.53±0.13. The zeta potential of the dispersed nanoparticles was recorded as −231±1.62 mV for the overall population, with Peak 1 corresponding to −32.79 mV. These parameters collectively indicate that the ball-milled *U. lactuca* particles exhibit a broad size distribution with high heterogeneity, where partial aggregation or agglomeration likely occurred during dispersion.

The Z-average of 728 nm suggests that the intensity-weighted mean particle size is within the submicron range. However, this parameter is highly influenced by the presence of larger particles, as the intensity of light scattering scales proportionally to the sixth power of the particle diameter (d^6) under the Rayleigh scattering regime (Hantke *et al*., 2018). Consequently, even though the measured Z-average appears relatively large, the presence of smaller nanoparticles

http://dx.doi.org/10.17844/qebg1c85

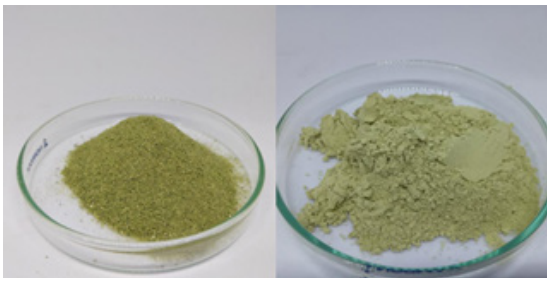

(A) (B)

Figure 4 *U. lactuca* powder (40 mesh) (A); Nanopowder (B)

Table 5 Particle size of nanopowder

Parameters	Standard (SNI 7383:2009) (mg/kg)
Size average (nm)	728.1±190.9
Peak 1 size (nm)	261±59.97
Peak 2 size (nm)	30.1±7.48
Polydispersity Index (PI)	0.53±0.13
Zeta potensial (mV)	-23.1±1.62

(<100 nm) can be masked by the dominant scattering signal from the larger aggregates (Stetefeld *et al*., 2016). In other words, a high Z-average value does not necessarily preclude the existence of nanosized primary particles but rather reflects a mixed system comprising nanoscale primary and aggregated entities.

The particle size distribution obtained from PSA displayed two prominent peaks at approximately 30 and 261 nm, signifying the coexistence of two distinct particle populations. The peak at approximately 30 nm likely represents primary nanosized particles generated through the high-energy mechanical milling process, whereas the 261 nm peak corresponds to secondary particles formed by the agglomeration of nanoscale fragments. This observation supports the interpretation that, although a fraction of the particles remains within the nanoscale range (<100 nm), aggregation and agglomeration phenomena contribute significantly to the overall intensity-weighted size. This behavior aligns with the known tendency of biopolymeric nanomaterials to form agglomerates owing to surface charge interactions and hydrogen bonding, particularly in hydrophilic matrices such as *Ulva lactuca*, which is rich in polysaccharides and proteins (Nemeth *et al.*, 2022). Hence, the PSA results suggest that ball milling produces a heterogeneous mixture of primary nanoparticles and larger agglomerated structures.

Furthermore, the PDI value of 0.53 indicates a polydisperse system, as PDI values greater than 0.3 typically denote a broad size distribution and non-uniformity in particle dispersion. This result implies that not all particles were evenly dispersed within the medium, and a significant fraction existed as loosely bound agglomerates. Meanwhile, the zeta potential of −23.1 mV reflects a moderately negative surface charge, sufficient to impart partial electrostatic repulsion among particles, although not strong enough to ensure long-term colloidal stability, which is commonly associated with absolute zeta potential values ≥30 mV. Therefore, the *Ulva lactuca* nanopowder exhibits intermediate electrostatic stability, indicating that although some electrostatic repulsion is present, the particles remain susceptible to agglomeration under changes in pH, ionic strength, or colloidal concentration (Nemeth *et a*l., 2022).

Taken together, the PSA data indicate that although the Z-average exceeds 100 nm, the presence of a distinct population peak at 30 nm confirms that a fraction of the particles falls within the nanoscale range. According to

the European Food Safety Authority (EFSA) (More *et al.*, 2021) and the International Organization for Standardization (ISO/TR 18401:2017), the classification of nanomaterials should not rely solely on intensity-based mean size but also on the number-based distribution and fraction of particles below 100 nm. Therefore, the PSA findings substantiate that the ball-milled *Ulva lactuca* material can be classified as a nanopowder, given the coexistence of primary nanosized particles and larger agglomerates formed during dispersion.

Nevertheless, to confirm the presence of nanoscale primary particles and visualize the interparticle boundaries, Scanning Electron Microscopy (SEM) and Transmission Electron Microscopy (TEM) analyses are required. These complementary techniques provide direct morphological evidence, surface structure details, and actual particle size distributions, thereby corroborating the PSA results. A detailed discussion of these findings is presented in the following section.

Scanning Electron Microscope (SEM)

SEM characterization was performed to observe the surface morphology of *Ulva lactuca* powder and nanopowder. The analysis of Scanning Electron Microscopy (SEM) images before and after the nanosizing process can describe the surface morphology and microstructure of the samples in detail through various magnifications (500×, 5,000×, and 10,000×), which are presented in Figures 5 and 6.

Scanning electron microscopy (SEM) analysis revealed a significant morphological difference between *Ulva lactuca* in powder and nanopowder forms. In the powder sample, SEM micrographs (at 500×, 5000×, and 10,000× magnifications) exhibited a relatively compact and layered surface structure, which retained fragments of cellulose polysaccharide sheets that were not completely degraded. This morphology reflects the natural characteristics of *Ulva lactuca*, which is rich in a matrix of ulvan polysaccharides, cellulose microfibrils, and structural proteins (Putra *et al.*, 2024). This morphology is consistent with the SEM results reported in a study of ulvan extraction from *U. fasciata*, where researchers also found an amorphous architecture characterized by particle aggregation and high porosity due to calcium bonds that are difficult to break (Moustafa *et al.*, 2024).

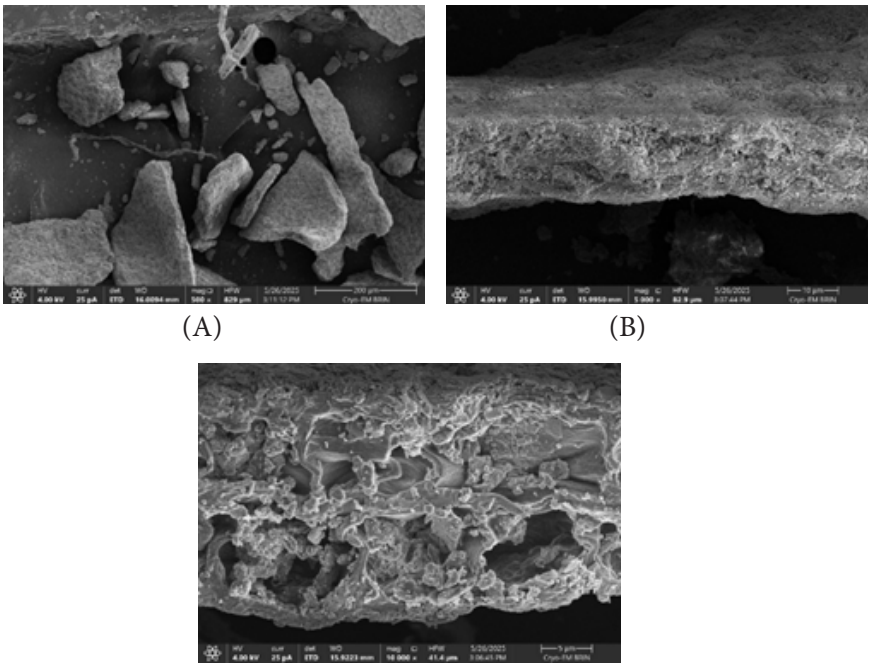

(A) (B)

(C)

Figure 5 Microstructure of *Ulva lactuca* powder observed by SEM at magnification; 500× (A), 5,000× (B), 10,000× (C)

http://dx.doi.org/10.17844/qebg1c85

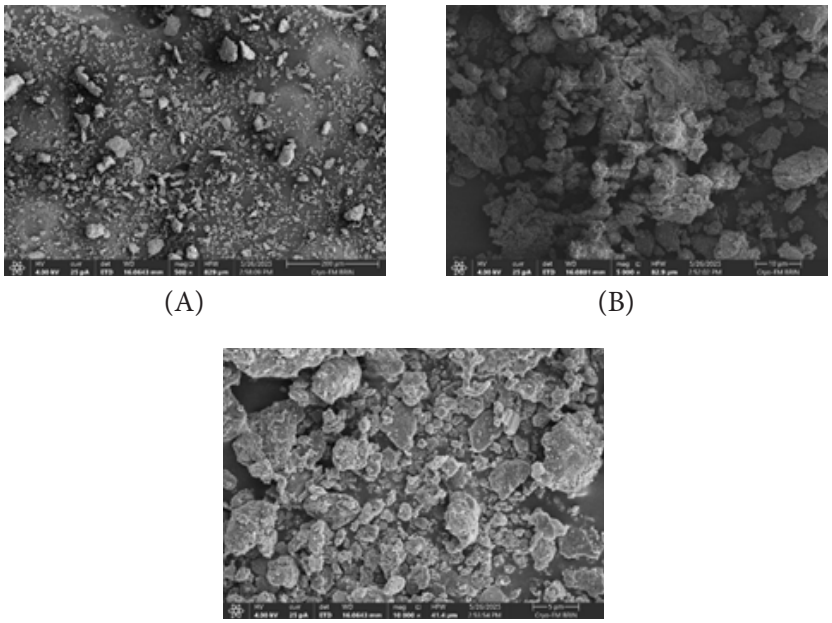

(A) (B)

(C)

Figure 6 Microstructure of *Ulva lactuca* nanopowder observed by SEM at magnification; 500× (A), 5,000× (B), 10,000× (C)

Conversely, the SEM micrographs of the nanopowder produced through ball milling showed a more porous and irregular surface, composed of micro-to-sub-micrometer-sized fragments, indicating intense mechanical degradation. These fragments formed loosely bound agglomerates with a rough texture and fine protrusions on their surfaces. This observation suggests the formation of primary nanoparticles that subsequently aggregate into larger clusters (agglomerates), as further supported by Particle Size Analysis (PSA) results showing two major peaks at 30 nm and 261 nm, with a Z-average diameter of 728 nm. This relationship confirms that the larger particle size detected by PSA mainly originates from the aggregation of nanoscale primary particles rather than from inherently large individual particles (More *et al*., 2021). Such behavior is commonly observed in biomaterials subjected to dry ball milling, where high-impact collisions generate nanoparticles that tend to re-agglomerate owing to the elevated surface energy, which is often driven by Van der Waals forces or hydrogen bonding (Nemeth *et al*., 2022).

The morphological transformation induced by planetary ball milling is also correlated with an increase in the specific surface area and disruption of cell wall structures, thereby enhancing the solvent accessibility of bioactive components such as polysaccharides, proteins, and photosynthetic pigments. Ibrahim *et al*. (2022) reported microstructural observations where cell wall degradation and increased extractability of ulvan were associated with mechanical treatments. Several studies on biomass ball milling (Wang *et al*., 2021; Mohamed *et al*., 2023) have documented that high-energy milling reduces particle size, introduces surface defects, and increases surface area, while sometimes promoting partial depolymerization of polysaccharides.

From a chemical perspective, the mechanochemical processes occurring during milling may lead to the cleavage of glycosidic bonds within the ulvan and cellulose chains, producing low-molecular-weight oligosaccharide fragments (Nemeth *et al*., 2022). This degradation improves solubility and enhances particle reactivity toward polar solvents, supporting its functional application in food and pharmaceutical systems.

Overall, the SEM comparison demonstrated that the ball milling process effectively altered the morphology of *Ulva lactuca* particles into a more porous and

heterogeneous structure, indicating the formation of nanoscale primary particles aggregated into agglomerates. These findings align with the PSA results, which show a bimodal size distribution (30 nm and 261 nm) and a zeta potential value of – 23, 1 mV, indicating moderate electrostatic stability. Thus, the resulting nanopowder morphology reflects the typical characteristics of biomass-derived nanomaterials, consisting of nanoscale primary particles physically joined into agglomerated structures. According to the European Commission (2011/696/EU) and EFSA (2021) definitions, this material can be classified as a "nano structured agglomerate" and should be functionally evaluated as a nanomaterial.

Transmission Electron Microscopy (TEM)

The analysis of Transmission Electron Microscopy *(TEM)* images before and after the ball milling process can explain the surface morphology and microstructure of the samples in detail through various magnifications, as presented in Figures 7 and 8.

In the *U. lactuca* powder sample revealed a layered lamellar structure with large fragments and cellulose fibril networks embedded within the ulvan polysaccharide matrix. The contrast variations, both high and low, indicate compositional heterogeneity between the crystalline (cellulose) and amorphous (ulvan and structural protein) domains. This observation is consistent with the findings of Piras *et al.* (2019), who reported that cellulose chains can organize into either irregular amorphous regions or highly ordered crystalline structures. This morphology indicates that the cell wall integrity remains largely preserved and has not undergone significant structural disruption due to the initial mechanical grinding. The lamellar and fibrillar architectures observed in this study are comparable to those described by Wahlstrom *et al.* (2020), who demonstrated that the *Ulva lactuca* cell wall consists of randomly oriented cellulose fibrils embedded in an amorphous ulvan matrix. Similar fibrillar arrangements are commonly found in green macroalgae, where they contribute to the rigidity and mechanical stability of the cell walls (Pari *et al.*, 2025).

Conversely, the TEM micrographs of the nanopowder sample exhibited pronounced morphological changes. The previously intact lamellar structures in the powder were fragmented into smaller particles ranging from several tens to hundreds of nanometers, suggesting that the ball milling process effectively caused cell wall disintegration and disruption of the internal fibrillar network of the cellulose. The high-contrast regions indicate the presence of spherical particles sized 20–80 nm and loosely aggregated clusters (200–300 nm), representing agglomerated primary nanoparticles. The appearance of fine pores and internal voids in the TEM images demonstrates intraparticle porosity, which can enhance the surface area and facilitate solvent diffusion during bioactive extraction (Ganeshan *et al.*, 2025). Such porosity not only accelerates extraction processes but can also shorten enzymatic reaction times for polysaccharides (Qu *et al.*, 2017). These findings support the PSA results, which show a bimodal size distribution (30 nm and 261 nm) with a Z-average of 728 nm and a PDI of 0.53.

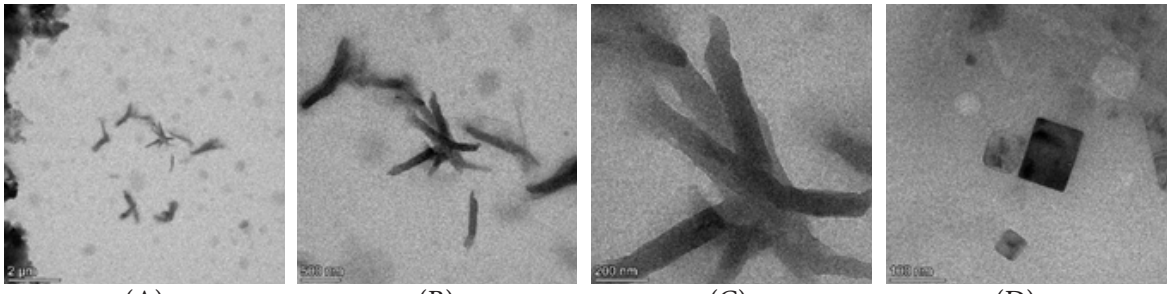

(A) (B) (C) (D)

Figure 7 TEM analysis of *Ulva lactuca* powder; 5,100× (A), 16,500× (B), 54,000× (C), 110,000× (D)

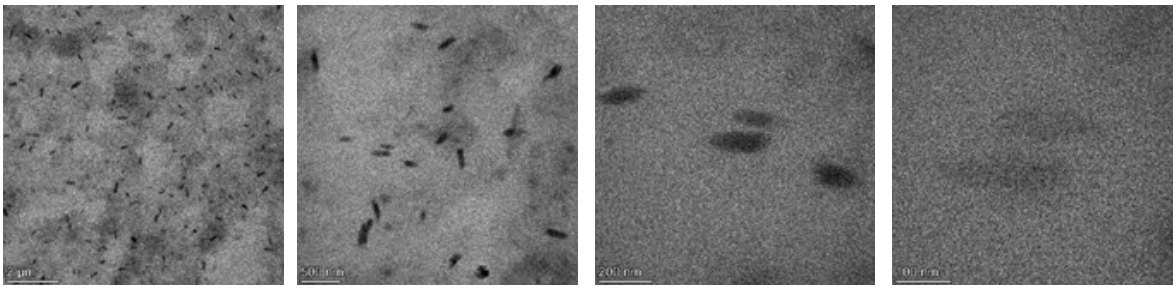

(A) (B) (C) (D)

Figure 7 TEM analysis of *Ulva lactuca* nanopowder; 5,100× (A), 16,500× (B), 54,000× (C), 110,000× (D)

This suggests that the nanopowder consists of nanometer-scale primary particles weakly bound together into larger aggregates by Van der Waals forces and hydrogen bonding among ulvan and cellulose molecules (Nemeth *et al*., 2022). Comparable results have been reported in studies on *Turbinaria* (Mohamed *et al*., 2023) and *Ulva* (Madany *et al*., 2021), where planetary ball milling transformed fibrous or sheet-like structures into nanoscale spheroidal fragments, increased porosity, and reduced the polysaccharide molecular weight.

Chemically, the morphological transformation observed in the nanopowder also indicates a mechanochemical effect, whereby the impact energy during ball milling breaks glycosidic bonds in ulvan and cellulose, yielding more soluble oligomeric fragments. The thin lines or short rod-like fragments observed under TEM may represent cellulose nanofibrils generated through mechanical cleavage (Piras *et al*., 2019). Similarly, Li *et al*. (2023) reported that ulvan appears as an amorphous matrix occupying inter-fibrillar spaces and that mechanical treatment facilitates the release of oligosaccharide fragments.

CONCLUSION

This study demonstrates that the particle size reduction of *Ulva lactuca* using planetary ball milling induces notable physicochemical and structural modifications without compromising the integrity of its main polysaccharide functional groups. Nanopowder formation led to changes in morphology and composition, which are associated with the improved accessibility of bioactive components, particularly proteins and amino acids. Despite these transformations, the overall chemical stability of the biomass was maintained and heavy metal levels remained within acceptable limits. Collectively, these findings indicate that *Ulva lactuca* nanopowder represents a promising functional raw material for potential applications in the food, pharmaceutical, and marine biotechnology sectors.

ACKNOWLEDGMENTS

The authors would like to thank the National Research and Innovation Agency (BRIN) and the Education Fund Management Agency (LPDP) through the Research and Innovation for Advanced Indonesia (RIIM) funding program RIIM competition scheme with contract number: 92/IV/KS/10/2024 and B.5986/POLTEK. AUP/KS.320/X/2024 dated 01 October 2024 in the name of the chief researcher Dr. Niken Dharmayanti, A.Pi., M.Si.

REFERENCES

Akbar, S. A., Lestari, A. N., Fazli, R. R., & Gunawan, G. (2025). Harnessing macroalgae for heavy metal phytoremediation:a sustainable approach to aquatic pollution control. *Bio Web of Conferences*, 156. https://doi.org/https://doi.org/10.1051/bioconf/202515602013

[BSN] Badan Standardisasi Nasional. (2006). SNI 01-2354.4-2006. Penentuan kadar protein metode *Kjedah*l total pada produk perikanan. Badan Standardisasi Nasional.

[BSN] Badan Standardisasi Nasional. (2009). SNI 7387:2009. Batas maksimum

cemaran logam berat dalam pangan. Badan Standardisasi Nasional.

[BSN] Badan Standardisasi Nasional. (2010). SNI 2354.1:2010. Cara uji kimia-bagian 1: penentuan kadar abu dan abu tak larut asam pada produk perikanan. Badan Standardisasi Nasional.

[BSN] Badan Standardisasi Nasional. (2015). SNI 01-2354.2-2015. Cara uji kimia kadar air pada produk perikanan. Badan Standardisasi Nasional.

[BSN] Badan Standardisasi Nasional. (2017). SNI 2354.3:2017. Cara uji kimia - bagian 3: pengujian kadar lemak total pada produk perikanan. Bandar Standardisasi Nasional.

Barakat, K. M., Ismail, M. M., Abou El Hassayeb, H. E., El Sersy, N. A., & Elshobary, M. E. (2022). Chemical characterization and biological activities of ulvan extracted from *Ulva fasciata* (Chlorophyta). *Rendiconti Lincei*, 33(4), 829–841. https://doi.org/10.1007/s12210-022-01103-7

Chen, J., Li, Y., & Liu, C. (2018). Influence of particle size reduction on ash content and mineral distribution in plant materials. *Journal of Food Engineering*, 223, 1–8.

Costa, J. F. da, Merdekawati, W., & Otu, F. R. (2018). Analisis proksimat, aktivitas antioksidan, dan komposisi pigmen *Ulva lactuca* dari perairan Pantai Kukup. *Jurnal Teknologi Pangan dan Gizi* (*Journal of Food Technology and Nutrition*), 17(1), 1–17.

Figueira, T. A., Silva, A. J. R. da, Enrich-prast, A., Yoneshigue-Valentin, Y., & Oliveira, V. P. de. (2020). Structural characterization of ulvan polysaccharide from cultivated and collected *Ulva fasciata* (Chlorophyta). *Advances in Bioscience and Biotechnology*, 11(5), 206–216. https://doi.org/10.4236/abb.2020.115016

Fithriani, D., Assadad, L., & Arifin, Z. (2017). Karakteristik dan model matematika kurva pengeringan rumput laut *Eucheuma cottonii*. *Jurnal Pascapanen dan Bioteknologi Kelautan dan Perikanan*, 11(2), 159. https://doi.org/10.15578/jpbkp.v11i2.290

Ganeshan, A., Periakaruppan, R., Vanathi, P., Thirumalaisamy, S. K., Selvaraj, K. S. V., & Moskovskikh, D. (2025). *Ulva rigida* – mediated silver nanoparticles : synthesis , characterization, and antibacterial activity. *Biomass Conversion and Biorefinery*, 15, 26605–26612. https://doi.org/10.1007/s13399-024-05440-5

Garcia, J., Moreira, B. R., Valverde-guill, P., Latorre-redoli, S., Caneda-santiago, C. T., Aci, G., Mart, E., Mar, M., & Abdala-d, R. T. (2023). In Vitro and In Vivo Effects of Ulvan Polysaccharides from *Ulva rigida*. *Pharmaceuticals*, 16(5), 660. https://doi.org/10.3390/ph16050660

Hantke, M. F., Bielecki, J., Kulyk, O., Westphal, D., Larsoon, D. S. ., Svenda, M., Reddy, H. K. ., Kirian, R. A., Andreasson, J., Hajdu, J., & Maia, F. R. N. (2018). Rayleigh-scattering microscopy for tracking and sizing nanoparticles in focused aerosol beams. *IUCrJ*, 5(Pt 6), 673–680. https://doi.org/10.1107/S2052252518010837

Hanutami, B., & Budiman, A. (2018). Review artikel: penggunaan teknologi nano pada formulasi obat herbal. *Farmaka*, 15(1), 37–46.

Hayati, R., Rahly, F., & Majid, M. I. (2023). Struktur genetik molekuler selada laut (*Ulva lactuca*) di Pantai Ulee Lheue, Indonesia. *Agroteknika*, 6(2), 249–261.

Heu, R., Shahbazmohamadi, Yorston, J., & Cadeper, P. (2021). Target material selection for sputter coating of SEM samples. *Microscopy Today*, 27(4), 32-36. https://doi.org/10.1017/S1551929519000610

Hofmann, L. C., Strauss, S., Shpigel, M., Guttman, L., Stengel, D. B., Rebours, C., Gjorgovska, N., Turan, G., Balina, K., Zammit, G., Adams, J. M. M., Ahsan, U., Bartolo, A. G., Bolton, J. J., Domingues, R., Dürrani, Ö., Eroldogan, O. T., Freitas, A., Golberg, A., … Meléndez-Martínez, A. J. (2024). The green seaweed Ulva: tomorrow's "wheat of the sea" in foods, feeds, nutrition, and biomaterials. *Critical Reviews in Food Science and Nutrition*, 65(19), 3728–3763. https://doi.org/10.1080/10408398.2024.2370489

Holdt, S. L., & Kraan, S. (2011). Bioactive compounds in seaweed : functional food applications and legislation. *Journal of Applied Phycologyl*, 23(3),543–597. https://doi.org/10.1007/s10811-010-9632-5

Hong, T., Yin, J., Nie, S., & Xie, M. (2021). Applications of infrared spectroscopy in polysaccharide structural analysis : Progress, challenge and perspective. *Food Chemistry,* 12, 100168. https://doi.org/10.1016/j.fochx.2021.100168

Ibrahim, M. I. A., Amer, M. S., Ibrahim, H. A. H., & Zaghloul, E. H. (2022). Considerable production of ulvan from *Ulva lactuca* with special emphasis on Its antimicrobial and anti-fouling properties. *Applied Biochemistry and Biotechnology*, 194(7), 3097–3118. https://doi.org/10.1007/s12010-022-03867-y

Indah, R. N., Saraswati, S. P. S., & Susilowati. (2021). Penyerapan logam magnesium dengan menggunakan bubuk alga merah (*Gracilaria* Sp). *Jurnal Teknik Kimia*, 15(2), 54–58. https://doi.org/10.33005/jurnal_tekkim.v15i2.2542

Jacoeb, A. M., Asnita, L., & Lingga, B. (2012). Karakteristik protein dan asam amino daging rajungan (*Portunus pelagicus)* akibat pengukusan. *Jurnal Pengolahan Hasil Perikanan Indonesia*, 15(2), 156–163.

Je, J.-G., Lee, H.-G., Fernando, K. H. ., Jeon, Y.-J., & Ryu, B. (2021). Purification and Structural Characterization of Sulfated Polysaccharides Derived from Brown Algae , *Sargassum binderi* : Inhibitory Mechanism of iNOS and COX-2 Pathway Interaction. *Antioxidants*, 10(6), 822. https://doi.org/10.3390/antiox10060822

Jiao, G., Yu, G., Zhang, J., & Ewart, H. S. (2011). Chemical structures and bioactivities of sulfated polysaccharides from marine algae. *Marine Drugs*, 9, 196–223. https://doi.org/10.3390/md9020196

Jung, H., Lee, Y. J., & Yoon, W. B. (2018). Effect of moisture content on the grinding process and powder properties in food : A Review. *Processes*. 6(6), 69. https://doi.org/10.3390/pr6060069

Khalid, W., Maggiolino, A., Kour, J., Arshad, M. S., Aslam, N., Afzal, M. F., Meghwar, P., Zafar, K., & Palo, P. De. (2023). Dynamic alterations in protein, sensory, chemical, and oxidative properties occurring in meat during thermal and non-thermal processing techniques : a comprehensive review. *Frontiers in Nutrition*, 9, 1057457. https://doi.org/10.3389/fnut.2022.1057457

Lam, H. S., Proctor, A., & Meullenet, J. (2001). Free fatty acid formation and lipid oxidation on milled rice. *Journal of the American Oil Chemists' Society*, 78, 1271-1275. https://doi.org/10.1007/s11745-001-0425-6

Li, C., Tang, T., Du, Y., Jiang, L., Yao, Z., Ning, L., & Zhu, B. (2023). Ulvan and ulva oligosaccharides : a systematic review of structure , preparation , biological activities and applications. *Bioresources and Bioprocessing*. 10(1), 66. https://doi.org/10.1186/s40643-023-00690-z

Liu, J., Lu, H., Wang, H., Mo, J., & Deng, Y. (2024). Mercury fractions transformation during sludge thermal treatment : implications for mercury release and stabilization in municipal sludge. *Journal of Soils and Sediments*, 24(11), 3750–3759. https://doi.org/10.1007/s11368-024-03920-9

Loh, Z. H., Samanta, A. K., & Heng, P. W. S. (2015). Overview of milling techniques for improving the solubility of poorly water-soluble drugs. *Asian Journal of Pharmaceutical Sciences*, 10(4), 255–274. https://doi.org/10.1016/j.ajps.2014.12.006

Madany, M. A., Abdel-kareem, M. S., Al-oufy, A. K., Haroun, M., & Sheweita, S. A. (2021). The biopolymer ulvan from *Ulva fasciata* : Extraction towards nano fibers fabrication. *International Journal of Biological Macromolecules*, 177, 401–412. https://doi.org/10.1016/j.ijbiomac.2021.02.047

Mao, X., Zeng, X., Qiao, S., Wu, G., & Li, D. (2011). Specific roles of threonine in intestinal mucosal integrity and barrier function. *Frontiers in Bioscience*, 6, 1192–1200.

Meiyasa, F., Ranjawali, E., Tuarita, M. Z., & Tarigan, N. (2023). Amino acid profile of Turbinaria ornata and *Ulva reticulata* from Moudolung Waters East Sumba. *Jurnal Pengolahan Hasil Perikanan Indonesia*, 26(3), 425–432. https://doi.org/10.17844/jphpi.v26i3.45699

Metwaly, H. R., El-Sayed, A. E. K. B., & Amin, H. F. (2023). Chemical and biochemical properties of marine algae *Ulva lactuca* and nannocholoropsis oculata. *Egyptian Journal of Aquatic Biology and Fisheries*, 27(3), 19–34. https://doi.org/10.21608/ejabf.2023.298840

Mohamed, A. A., Sameeh, M. Y., & El-Beltagi, H. S. (2023). Preparation of seaweed nanopowder particles using planetary ball milling and their effects on some secondary metabolites in date palm (*Phoenix dactylifera* L.) Seedlings. *Life*, 13(1). https://doi.org/10.3390/life13010039

Monks, J. L. F., Vanier, N. L., Casaril, J., Berto, R. M., de Oliveira, M., Gomes, C. B., de Carvalho, M. P., Dias, A. R. G., & Elias, M. C. (2013). Effects of milling on proximate composition, folic acid, fatty acids and technological properties of rice. *Journal of Food Composition and Analysis*, 30(2), 73–79. https://doi.org/10.1016/j.jfca.2013.01.009

Monteiro, C. A., Cannon, G., Lawrence, M., Louzada, M. L. da C., & Machado, P. P. (2019). Ultra-processed foods, diet quality , and health using the NOVA classification system. *Public Health Nutrition,* 22(5), 936-941. https://doi.org/10.1017/S1368980018003762

More, S., Bampidis, V., Benford, D., Bragard, C., Halldorsson, T., Bennekou, S. H., Koutsoumanis, K., Machera, K., Naegeli, H., Nielsen, S., Schlatter, J., Schrenk, D., Silano, V., Turck, D., Younes, M., Castenmiller, J., Chaudhry, Q., Cubadda, F., Franz, R., Schoonjans, R. (2021). Guidance on risk assessment of nanomaterials to be applied in the food and feed chain : human and animal health. *EFSA Journal*, *EFSA Journal*, 19(8), 1-48. https://doi.org/10.2903/j.efsa.2021.6768

Moreira, R., Sineiro, J., Chenlo, F., Arufe, S., & Díaz-Varela, D. (2017). Aqueous extracts of Ascophyllum nodosum obtained by ultrasound-assisted extraction: effects of drying temperature of seaweed on the properties of extracts. *Journal of Applied Phycology*, 29(6), 3191–3200. https://doi.org/10.1007/s10811-017-1159-6

Moustafa, M. H., Turkey, M. S., Mohamedin, N. S., Darwish, A. A., Elshal, A. A. M., Yehia, M. A. H., El Safwany, M. M., & Mohamed, E. I. (2024). Eggshell membrane and green seaweed (*Ulva lactuca*) micronized powders for in vivo diabetic wound healing in albino rats: a comparative study. *Journal of Pharmaceutical Health Care and Sciences*, 10(1), 1–14. https://doi.org/10.1186/s40780-024-00345-x

Nemeth, Z., Csoka, I., Jazani, R. S., Sipos, B., Haspel, H., Kozma, G., Konya, Z., & Dobo, D. G. (2022). Quality by design-driven zeta potential optimisation study of liposomes with charge imparting membrane additives. *Pharmaceutics*, 14(9), 1798. https://doi.org/10.3390/pharmaceutics14091798

Nufus, C., Nurjanah, & Abdullah, A. (2017). Karakteristik rumput laut hijau dari perairan kepulauan seribu dan sekotong Nusa Tenggara Barat sebagai antioksidan. *Jurnal Pengolahan Hasil Perikanan Indonesia*, 20(3), 620–632.

Pari, R. F., Uju, U., Hardiningtyas, S. D., Ramadhan, W., & Wakabayashi, R. (2025). Ulva seaweed-derived ulvan : a promising marine polysaccharide as a sustainable resource for biomaterial design. *Marine Drugs*, 23(2), 56. https://doi.org/10.3390/md23020056

Piras, C. C., Fernandez-Prieto, S., & Borggraeve, W. M. De. (2019). Nanoscale advances Ball milling : a green technology for the preparation and functionalisation of nanocellulose derivatives. *Nanoscale Advances*, 1(3), 937–947. https://doi.org/10.1039/c8na00238j

Patrichi, C. A. M., Cioroiu Tirpan, D. R., Aljanabi, A. A. A., Trica, B., Gifu, I. C., & Dobre, T. (2023). Extraction of cellulose

from *Ulva lactuca* algae and its use for membrane synthesis. *Polymers*, 15(24), 4673. https://doi.org/10.3390/polym15244673

Pratama, R. I., Rostini, I., & Awaluddin, M. Y. (2013). Komposisi kandungan senyawa Flavor ikan mas (*Cyprinus carpio*) segar dan hasil pengukusannya. *Jurnal Akuatika*, 4(1), 55–67.

Pratiwi, A. R., Fadlilah, I., Ananingsih, V. K., & Meiliana. (2021). Protein and amino acid of edible *Sargassum aquifolium*, *Ulva lactuca* and *Gracilariopsis longissima*. *Jurnal Pengolahan Hasil Perikanan Indonesia*, 24(3), 337–346. https://doi.org/10.17844/jphpi.v24i3.37085

Ptak, S. H., Sanchez, L., Fretté, X., & Kurouski, D. (2021). Complementarity of Raman and Infrared spectroscopy for rapid characterization of fucoidan extracts. *Plant Methods*, 17(1)130. https://doi.org/10.1186/s13007-021-00830-6

Putra, N. R., Fajriah, S., Qomariyah, L., Dewi, A. S., Rizkiyah, D. N., Irianto, I., Rusmin, D., Melati, M., Trisnawati, N. W., Darwati, I., & Arya, N. N. (2024). Exploring the potential of *Ulva Lactuca* : Emerging extraction methods, bioactive compounds, and health applications – A perspective review. *South African Journal of Chemical Engineering*, 47, 233–245. https://doi.org/10.1016/j.sajce.2023.11.017

Qu, T., Zhang, X., Gu, X., Han, L., Ji, G., Chen, X., & Xiao, W. (2017). Ball milling for biomass fractionation and pretreatment with aqueous hydroxide solutions. *ACS Sustainable Chemistry and Engineering*, 5(9), 7733–7742. https://doi.org/10.1021/acssuschemeng.7b01186

Ramadhan, W., Uju, Hardiningtyas, S. D., Pari, R. F., Nurhayati, & Sevica, D. (2022). Ultrasonic wave assisted extraction of ulvan polysaccharide from *Ulva lactuca* Seaweed at low temperature. *Jurnal Pengolahan Hasil Perikanan Indonesia*, 25(1), 132–142. https://doi.org/10.17844/jphpi.v25i1.40407

Rasyida, A., Pradipta, T. R., & Wicaksono, S. T. (2019). Studi pengaruh penambahan PVA dan bentonit terhadap morfologi dan sifat fisik komposit berbasis hidrogel alginat sebagai kandidat material perancah untuk regenarasi tulang rawan. *Jurnal Teknik ITS*, 7(2), F320-321. https://doi.org/10.12962/j23373539.v7i2.42611

Raya, I., & Rahmah, R. (2012). The bioaccumulation of Cd (ii) Ions on *Euchema Cottoni* seaweed bioakumulasi Ion Cd (ii) pada rumput laut *Euchema Cottoni*. *Jurnal Administrasi dan Kebijakan Kesehatan Indonesia,* 13(2), 109321.

Safitri, R. A. (2020). Pemanfaatan limbah kulit salak pondoh (*Salacca edulis*) sebagai komposit karbon aktif termodifikasi untuk adsorbsi logam timbal (Pb). [Skripsi]. Universitas Islam Indonesia.

Sailah, I., & Miladulhaq, M. (2021). Perubahan sifat fisikokimia selama pengolahan bawang putih tunggal menjadi bawang hitam menggunakan *rice cooker*. *Jurnal Teknologi Industri Pertanian*, 31(1), 88–97.

Sari, D. K., Lestari, R. S. D., & Rahmat, A. (2016). Biosintesis nano/mikro partikel perak dari rumput laut (*Eucheuma Cottonii*) berbantu gelombang ultrasonik. Seminar Nasional Sains dan Teknologi Fakultas Teknik Universitas Muhammadiyah Jakarta, November, 1–10. jurnal.umj.ac.id/index.php/semnastek

Shuuluka, D., Bolton, J. J., & Anderson, R. J. (2013). Protein content, amino acid composition and nitrogen-to-protein conversion factors of *Ulva rigida* and *Ulva capensis* from natural populations and *Ulva lactuca* from an aquaculture system, in South Africa. *Journal of Applied Phycology*, 25(2), 677–685. https://doi.org/10.1007/s10811-012-9902-5

Sianipar, E. A., Satriawan, N., Sumartono, J., & Kambira, P. F. A. (2022). Pengujian aktivitas antioksidan makro alga Sumbawa dalam hubungannya dengan kandungan senyawa bioaktif dan efek farmakologi. *Jurnal Riset Kesehatan Nasional*, 6(2), 151–157. https://doi.org/10.37294/jrkn.v6i2.457

Spínola, M. P., Costa, M. M., & Prates, J. A. M.

(2023). Effect of selected mechanical/ physical pre-treatments on *Chlorella vulgaris* protein solubility. *Agriculture*, 13(7), 1–13. https://doi.org/10.3390/agriculture13071309

Stetefeld, J., McKenna, S. A., & Patel, T. R. (2016). Dynamic light scattering: a practical guide and applications in biomedical sciences. *Biophysical Reviews*, 8(4), 409–427. https://doi.org/10.1007/s12551-016-0218-6

Tran, V. H. N., Mikkelsen, M. D., Truong, H. B., Vo, H. N. M., Pham, T. D., Cao, H. T. T., Nguyen, T. T., Meyer, A. S., Thanh, T. T. T., & Van, T. T. T. (2023). Structural characterization and cytotoxic activity evaluation of ulvan polysaccharides extracted from the green algae. *Marine Drugs*. 21(11), 556. https://doi.org/https://doi.org/10.3390/md21110556

Vassilev, S. V, Vassileva, C. G., Georgieva, M. G., Barbov, B. Z., Velyanova, G. G., & Georgiev, S. V. (2024). Content, association and potential modes of occurrence of mercury in diverse biomass types and their ecological significance. *Geologica Balcanica*, 53(2), 69–87.

Veeraswamy, D., Subramanian, A., Mohan, D., Ettiyagounder, P., Selvaraj, P. S., Ramasamy, S. P., & Veeramani, V. (2023). Exploring the origins and cleanup of mercury contamination : a comprehensive review. *Environmental Science and Pollution Research*, 31(41), 53943-53972. https://doi.org/10.1007/s11356-023-30636-z

Wahlstrom, N., Edlund, U., Pavia, H., Toth, G., Jaworski, A., Pell, A. J., Choong, F. X., Hamid, S., Nilsson, K. P. R., & Richter-dahlfors, A. (2020). Cellulose from the green macroalgae *Ulva lactuca* : isolation, characterization, optotracing, and production of cellulose nanofibrils. 27(7), 3707-3725.. https://doi.org/10.1007/s10570-020-03029-5

Wang, Z., Zhu, X., & Deuss, P. J. (2021). The effect of ball milling on birch , pine , reed , walnut shell enzymatic hydrolysis recalcitrance and the structure of the isolated residual enzyme lignin. *Industrial Crops & Products*, 167, 113493. https://doi.org/10.1016/j.indcrop.2021.113493

Wang, D., Liu, Y., & Guo, M. (2024). Effect of ball-milling treatment combined with glycosylation on the structure and functional properties of *Litopenaeus vannamei* protein. *Foods*, 13(9), 1284. https://doi.org/https://doi.org/10.3390/foods13091284

Zhao, S., Pan, Z., Azarakhsh, N., Ramaswamy, H. S., Duan, H., & Wang, C. (2024). Effects of high-pressure processing on the physicochemical and adsorption properties, structural characteristics , and dietary fiber content of kelp (*Laminaria japonica*). *Current Research in Food Science*, 8, 100671. https://doi.org/10.1016/j.crfs.2023.100671

Zheng, Y., Fu, Z., Li, D., & Wu, M. (2018). Effects of ball milling processes on the microstructure and rheological properties of microcrystalline cellulose as a sustainable polymer additive. *Materials*, 11(7), 1057. https://doi.org/10.3390/ma11071057

Zhou, L., Sui, Y., Zhu, Z., Li, S., Xu, R., Wen, J., Shi, J., Cai, S., Xiong, T., Cai, F., & Mei, X. (2023). Effects of degree of milling on nutritional quality, functional characteristics and volatile compounds of brown rice tea. *Frontiers in Nutrition*, 10, 1232251. https://doi.org/10.3389/fnut.2023.1232251